



Fibers with Polyisoprenes from Jackfruit Latex (*Artocarpus heterophyllus* L.) by Electrohydrodynamic Processes: Fabrication and Characterization

Dania Marlene Ceballos-Vázquez¹ , Montserrat Calderón-Santoyo^{1,2} ,
Elda Margarita González-Cruz³ , Cristina Prieto⁴ , José María Lagarón⁴, Juan Arturo Ragazzo-Sánchez^{1,2*} 

¹ Integrated Food Research Laboratory, National Technological Institute of Mexico/Technological Institute of Tepic, Avenue. Tecnológico #2595, Lagos del Country, Tepic, Nayarit, C.P. 63175, Mexico; damaceballosva@ittecip.edu.mx (D.M.C.V.); arturoragazzo@hotmail.com, jragazzo@ittecip.edu.mx (J.A.R.S.); mcalderon@tepic.tecnm.mx (M.C.S.)

² Department of Agricultural, Food and Nutritional Science, University of Alberta, Edmonton, AB T6G 2P5, Canada. ragazzos@ualberta.ca (J.A.R.S.); montser1@ualberta.ca (M.C.S.);

³ Department of Graduate Studies and Research, National Technological Institute of Mexico/Technological Institute of Tlajomulco, Km 10 carr Tlajomulco, Cto. Metropolitano South, 45640 Tlajomulco de Zuñiga, Jal. Mexico; elda051194@gmail.com (E.M.G.C.);

⁴ Novel Materials and Nanotechnology Group, Institute of Agrochemistry and Food Technology (IATA), Spanish Council for Scientific Research (CSIC), Calle Catedrático Agustín Escardino Benlloch 7, 46980 Paterna, Spain; cprieto@iata.csic.es (C.P.); lagaron@iata.csic.es (J.M.L.);

* Correspondence: arturoragazzo@hotmail.com, jragazzo@ittecip.edu.mx;

Scopus Author ID 8207779900

Received: 9.06.2023; Accepted: 7.08.2023; Published: 4.02.2024

Abstract: This investigation aims to evaluate the feasibility of polyisoprenes from jackfruit latex (pure or combined with PEO or pullulan) to form fibers by electrospinning process. The pH, conductivity, and surface tension of the polyisoprene concentrate (PC) solutions and dispersions are evaluated. The electrospun nanofibers are characterized by SEM, ATR-FTIR, thermal analysis, solubility, and water vapor transmission rate (WVTR). According to the physicochemical characteristics, the solutions are suitable for electrospinning. Fibers by electrospinning are obtained from all solutions (PEO/Pullulan + 0.2, 0.5, or 1% PC). ATR-FTIR spectrum of the nanofibers presents no differences with the presence of PC, suggesting that the interactions between the polymers are not covalent, which facilitates PC release. Nanofibers present homogeneous and continuous morphology, with diameters ranging from 200-400 nm with pullulan and 100-300 nm with PEO. Nanofibers show no statistical difference in the solubility parameter and present low WVTR values. Thermal analysis shows compatibility between polymers and the increase of thermal stability of PC when mixed with pullulan or PEO. Therefore, the PC-based nanofibers could be used for the encapsulation of bioactive molecules or in the development of dermal products based on the biological activities that have been attributed to polyisoprenes.

Keywords: jackfruit; latex; polyisoprenes; electrospinning; nanofibers.

© 2024 by the authors. This article is an open-access article distributed under the terms and conditions of the Creative Commons Attribution (CC BY) license (<https://creativecommons.org/licenses/by/4.0/>).

1. Introduction

Artocarpus heterophyllus Lam. (Jackfruit) is a latex-producing plant. Jackfruit latex is an exudate from all parts of the plant produced by secretory cells called laticifers and is considered an agro-industrial waste in producing this fruit [1,2]. Traditionally, latex from different species has been used as a wound healing agent, either applied directly in the wound

or as a biomembrane [3–7]. Latex comprises lipids, sugars, proteins, enzymes, and rubber [8]. However, the role of each individual component of the latex in wound healing is not well established. Even though latex composition varies from plant to plant, one of the most common compounds found in latex originates from isoprene units and belongs to the class of terpenes. The most important terpene in latex is rubber (*cis*-1,4-polyisoprene) [9]. Li *et al.* [10] found that *trans*-polyisoprene nanoparticles could stimulate the synthesis of some proteins that promote cell growth, improving the healing process, which suggests that polyisoprenes might be one of the active components that promote wound healing. Bhadra *et al.* [11] reported that jackfruit rubber contained *cis*-1,4-polyisoprene (34.4%) and *trans*-1,4-polyisoprene (65.6%). Polyisoprenes are constituted by isoprene molecules of five carbons (2-methyl-1,3-butadiene); according to Bhadra *et al.* [11], the polyisoprenes in jackfruit latex could have molecular weights from 5000 to 10000 g/mol. Ramos-Martínez *et al.* [8] reported that polyisoprenes of low molecular weight from jackfruit latex have techno-functional properties, such as emulsifying and foaming activity, and thermal stability.

Although polyisoprenes have wide applications, the low solubility of polyisoprene limits the applications. A solution to overcome this drawback is to use a delivery system, such as nanofibers obtained by the electrospinning process, which has proved to enhance solubility [12]. Electrospinning is a versatile method used to produce continuous fibers with diameters ranging from nanometers to micrometers. The nanofibers obtained are long polymeric filaments with a large surface area, porosity, and elasticity [13]. Nevertheless, the low glass transition temperature of polyisoprenes complicates the handling and stabilization during electrohydrodynamic processes (<100°C) [11]. A viable alternative to be used in the electrospinning process is to combine them with other polymers [8]. Polymeric materials such as pullulan and polyethylene oxide (PEO) have been shown to function as co-spinning polymers to improve electro-stability [14,15]. Pullulan is an extracellular polysaccharide produced by the fungus *Aureobasidium pullulans*. It is an edible, non-toxic, non-mutagenic, non-immunogenic neutral glucan [16]. The linear structure of pullulan confers flexibility, good water solubility, and the ability to form fibers [17]. PEO is a widely used polymer due to its semi-crystalline state, biocompatibility, biodegradability, and water-solubility. Recently, PEO developed an interest in the pharmaceutical industry for the controlled release of solid-dose matrix systems, transdermal drug delivery devices, and mucosal bio-adhesives [18,19].

Polyisoprenes (*-cis* and *-trans*) with high molecular weight have been used to form fibers in electrohydrodynamic processes, specifically in electrospinning mode [20–24]. However, there are no studies of nanostructure formation (capsules/fibers) of low molecular weight *-cis* or *-trans* polyisoprenes by electrospinning. Therefore, using polyisoprenes from jackfruit latex in developing dermal products could be an alternative to valorize this by-product.

This study aimed to evaluate the feasibility of forming fibers of polyisoprene (pure or in combination with other polymeric materials) from jackfruit latex, which could have potential dermic biomedical applications, providing value to agro-industrial waste without current use.

2. Materials and Methods

2.1. Plant material.

Latex was collected during the harvest of jackfruit (*Artocarpus heterophyllus* L.) from crops located in Zacualpan, Nayarit (21°19'09.0' N 105°10'15.7' W). Ammonium hydroxide 1% (v/v) was added as a preservative during transport and maintained at 4°C until use.

2.2. Chemicals.

Polyethylene oxide (PEO) (Mw ~ 400,000 Da), Tween 20, and pepsin (EC 3.4.23.1) were purchased at Sigma Aldrich (St. Louis, MO, USA). Pullulan (Mw ~ 2x10⁵ Da) was acquired at Hayashibara CO., LTD. (Tokyo, Japan). Sodium hydroxide (NaOH), hydrochloric acid (HCl), sulfuric acid (H₂SO₄), sodium lauryl sulfate (C₁₂H₂₅NaO₄S) ammonium hydroxide (NH₄OH), and dichloromethane were obtained from Jalmek (Nuevo León, México). All chemicals used were reagent grade.

2.3. Polyisoprene extraction.

Polyisoprene extraction was performed according to the methodology reported by Ramos-Martínez *et al.* [8]. Jackfruit latex (500 mL) was mixed with sodium lauryl sulfate (SLS) in a 1:1 ratio (w/w). The sample was deproteinized by adding 0.014% (w/v) pepsin previously activated in 0.5 ml of distilled water at pH 2.0. It was maintained at 37°C for 3 h under magnetic stirring at 750 rpm, followed by two centrifugation cycles (22,598 g for 15 min, 15°C), replacing the supernatant with distilled water. The resulting material was saponified with a 2% (w/v) sodium hydroxide solution in a 2:1 ratio (NaOH:sample) and incubated for 3 h at 70°C in a water bath. Finally, two centrifugation cycles (22,598 g for 15 min, 15°C) were performed to remove saponifiable lipids.

2.4. Polymeric solutions and dispersions preparation.

A PC solution at 1.6% (w/w) in dichloromethane was prepared and homogenized for 30 min under magnetic stirring at 300 rpm. A 20% (w/w) pullulan and a 5% (w/w) PEO of total solids solutions were also prepared. The polymers were separately dissolved in distilled water and homogenized for 6 h with magnetic stirring at 300 rpm. Tween 20 was added as a surfactant at a concentration of 1% (w/w) for both solutions.

Subsequently, PC was incorporated into polymeric dispersions at different concentrations (1, 0.5, and 0.2% w/w) concerning the aqueous solutions of pullulan and PEO previously prepared. Solutions were heated at 70°C with magnetic stirring at 300 rpm for 10 min to enhance PC suspension. All solutions were processed immediately after preparation.

2.5. Physicochemical characterization of polymeric solutions and dispersion.

Conductivity and pH of the polymeric solutions/dispersions were measured using Hanna Instruments multiparameter potentiometer HI 251 (Rhode Island, USA) at 25° C. Surface tension was determined by the Wilhemy plate method on an EasyDyne K20 tensiometer (Krüss GmbH, Hamburg, Germany). All measurements were performed in triplicate (*n*=3).

2.6. *Nanofibers obtained by electrospinning process.*

The polymeric suspensions/dispersions were processed by electrospinning in Fluidnatek LE-10 equipment (Bioinicia, Valencia, Spain). Electrospinning conditions to obtain fibers were 0.1 mL h⁻¹ of flow rate, 11 kV in the needle, and a distance between the needle tip and collector of 20-30 cm. Produced fibers were stored in a desiccator for subsequent analysis.

2.7. *Morphology and size distribution of the structures.*

Fiber morphology was determined using a scanning electron microscopy Hitachi-S-4800 FE-SEM (Hitachi High-Technologies Corporation, Tokyo, Japan) with acceleration of 5 kV. Approximately 1 mg of the sample was fixed on a double-sided adhesive tape and placed on a metal slide. Subsequently, the sample was coated with gold-palladium for 2 min. Fiber size was analyzed using Image J software v1.41 (National Institutes of Health, Bethesda, USA), and the data presented were obtained from a minimum of 100 fibers.

2.8. *Attenuated Total Reflectance Fourier Transform Infrared Spectroscopy analysis.*

The wavelengths at which different bonds/functional groups of polyisoprenes, pullulans, and PEO vibrate were analyzed by attenuated total reflectance (ATR)-Fourier transform infrared spectroscopy (FTIR). Approximately 1 mg of the sample was placed in the spectrophotometer (Bruker FTIR Tensor 37, Rheinstetten, Germany). All the spectra were obtained within the wavenumber range of 4,000-600 cm⁻¹ by averaging 10 scans at 4 cm⁻¹ resolution.

2.9. *Solubility determination of the nanofibers.*

Solubility was determined according to the solvation method reported by Jiménez-Sánchez *et al.* [25]. First, 0.1 g of nanofibers were diluted in 10 mL of distilled water. Subsequently, the sample was centrifuged at 3,000 g for 5 min. An aliquot of 2 mL of the supernatant was taken, placed in Petri dishes, and dried in an oven (EI60-AID, Novatech, Mexico) at 105°C until constant weight was reached. Solubility percent (%) was calculated according to equation 1.

$$\% \text{ solubility} = \frac{\text{solid weight} * 5}{\text{sample weight}} \times 100 \quad (1)$$

Where solid weight corresponds to the weight of the sample after solubilization (g), sample weight is the initial weight of the sample (g).

2.10. *Water vapor transmission rate (WVTR) of nanofibers.*

The WVTR was measured gravimetrically according to the methodology of Gonzalez-Estrada *et al.* [26]. The permeation cell with distilled water (100% RH; 2337 Pa vapor pressure at 20°C) was sealed with the fibers, placed in a desiccator at 20°C and 0% RH (0 Pa vapor pressure of water) with silica for moisture control. Cells were weighed every 24 h until a constant weight was reached. The slope of the loss as a function of time was obtained by linear regression. The WVP and WVTR of the fibers were determined according to equation 2.

$$WVTR = \frac{\text{slope}}{\text{Area}} \quad (2)$$

2.11. Thermal analysis of nanofibers.

Thermogravimetric analysis of the polyisoprenes extract, polymers, and nanofibers was performed on a TGA 550, TA Instruments (New Castle, DE, USA). In a platinum crucible, 5 mg of sample were placed, using a heating ramp from 25 to 800°C, at a rate of 5°C min⁻¹ in an atmosphere of N₂. Differential scanning calorimetry analysis was executed in a DSC 250, TA Instruments (New Castle, DE, USA). In a hermetically sealed aluminum crucible, 5 mg of sample was placed, and a ramp with heating and cooling cycles was used to identify the glass transition temperature and other thermal events. The first cycle was set from 25 to 100°C, the second from 100 to -45°C, and the third from -45 to 400°C, with a heating rate of 5°C min⁻¹ under a N₂ atmosphere. Interpretation of TGA and DSC thermal analysis results was effectuated using TRIOS software (TA Instruments, New Castle, DE, USA).

2.12. Statistical analysis.

The data obtained from the physicochemical characterization of the solutions, solubility, and water vapor transmission rate of the electrospun fibers were expressed as the mean ± standard deviation of three replicates and analyzed by one-way ANOVA test. Statistical differences were assessed by Tukey's comparison of means test with p<0.05. STATISTICA 12 software (Tibco, California USA) was used for the statistical analysis.

3. Results and Discussion

3.1. Physicochemical characteristics of PC solutions and dispersions.

The physicochemical characteristics of polymeric solutions determine the susceptibility of the solution to be electrospun. To start the electrospinning process, it is essential to overcome the surface tension of the solution [27]; therefore, low values of surface tension (<80 mN m⁻¹) are preferred [28]. The conductivity favors charge migration to the surface, which is necessary to suppress the surface tension to initiate the electrospinning process [29]. When the conductivity parameter is greater than 5 mS cm⁻¹, high voltage values must stabilize the process [28]. Therefore, intermediate conductivity values (0.2 to 5 mS cm⁻¹) are preferred. The PC solution in dichloromethane presented low values of conductivity (1.79 ± 0.2 μS cm⁻¹) and surface tension (27.8 ± 0.0 mN m⁻¹), associated with the physicochemical characteristics of dichloromethane, which has a low surface tension (27.12 mN m⁻¹) and conductivity (0.2 μS cm⁻¹). Nie *et al.* [22] reported similar values of surface tension (26.81 mN m⁻¹) and conductivity (0.94 ± 0.2 μS cm⁻¹) of trans-polyisoprenes solutions in a mixture of N,N-dimethylformamide (Conductivity: 2.5 μS cm⁻¹; surface tension: 37.1 mN m⁻¹) and chloroform (Conductivity: 2×10⁻⁸ S m⁻¹; surface tension: 27.1 mN m⁻¹), attributed likewise to the low conductivity and surface tension of the solvents used.

Pullulan dispersions with PC showed a significant difference (p<0.05) in the conductivity parameter (Table 1). Ascending behavior was observed in the conductivity of the dispersions as a function of PC concentration; this phenomenon could be related to the presence of salts and minerals in the polyisoprene concentrate [8]. Moreover, the heating of the solutions could have also improved the conductivity value; this behavior could be attributed to the polymer-polymer interactions by forming hydrogen bridges, which modifies the electrical charge of pullulan solutions and facilitates the electrospinning process. The increase of conductivity value in pullulan solutions when combined with other substances, such as proteins

or polysaccharides, has been reported previously by Jia *et al.* [30] and Ponrasu *et al.* [31]; the authors mention that this increase in conductivity enhances the stability of the electrospinning process. PEO dispersions with PC presented relatively low conductivity values and no significant difference between the dispersions (Table 1). Despite the low conductivity values, Peinado *et al.* [18] reported that PEO has high electrostability and requires low voltages to be electrospun (5-15 kV). This behavior differs from that presented by pullulan dispersions, associated with pullulan structure and its easiness to form hydrogen bonding, which improves conductivity, whereas PEO tends to interact with other polymers via hydrophobic and hydrophilic interactions [32].

Table 1. Physicochemical properties of polymeric dispersions for the electrospinning process.

Sample	PC (%)	Conductivity ($\mu\text{S}/\text{cm}$)	Surface Tension (mN/m)	pH
PUL	0	31.1 ± 1.5^a	40.6 ± 0.3^a	4.2 ± 0.2^a
PUL-PC	1	198.4 ± 3.2^b	40.4 ± 0.2^a	3.6 ± 0.4^a
PUL-PC	0.5	134.2 ± 1.3^c	40.0 ± 0.4^a	3.7 ± 0.5^a
PUL-PC	0.2	69.1 ± 2.4^d	40.1 ± 0.3^a	3.8 ± 0.3^a
PEO	0	76.7 ± 2.0^a	41.8 ± 0.1^a	6.1 ± 0.5^a
PEO-PC	1	72.5 ± 1.2^b	41.6 ± 0.3^a	7.6 ± 0.4^b
PEO-PC	0.5	73.8 ± 1.0^b	41.9 ± 0.2^a	7.5 ± 0.8^b
PEO-PC	0.2	74.0 ± 1.2^b	41.8 ± 0.2^a	7.8 ± 0.4^b

*Different letters per column and polymer indicate statistical differences ($p < 0.05$).

Even though Ramos-Martinez *et al.* [8] reported that low molecular weight polyisoprenes from jackfruit latex exhibit emulsifying properties, no significant difference ($p > 0.05$) was observed in the surface tension values in any of the polymer dispersions (Table 1), this behavior could be attributed to the low ratios of PC incorporated.

The dispersions of pullulans with PC did not present statistical differences ($p > 0.05$) in the pH values (Table 1) associated with the low concentration of PC. There was a statistical difference between the PEO and PEO-PC dispersions; the increase in pH could be related to the lipophilic character of the sample. It is worth mentioning that the neutrality of the solutions, as well as neutral fibers, favor their dermal application [33].

3.2. Morphology and size of nanofibers.

The formation of fibers of PC dissolved in dichloromethane by electrospinning was possible. Continuous ribbon-shaped fibers without ruptures were obtained. In addition, the loss of fiber's initial shape until it is flattened on the surface is detected (Figure 1). This phenomenon could be related to the environmental conditions in which the process was developed (26°C and 56% relative humidity); Nie *et al.* [22] attributed this issue to the glass transition temperature, which is below room temperature (-65°C), causing the structures to lose their shape after reaching the collector, forming flat films. Fiber morphology is similar to the reported by Chen *et al.* [20], who used 1% of high molecular weight *trans*-polyisoprenes for fiber formation by electrospinning. However, it should be noted that this is the first time that fiber formation has been achieved using low molecular weight *cis* and *trans* polyisoprenes from jackfruit latex.

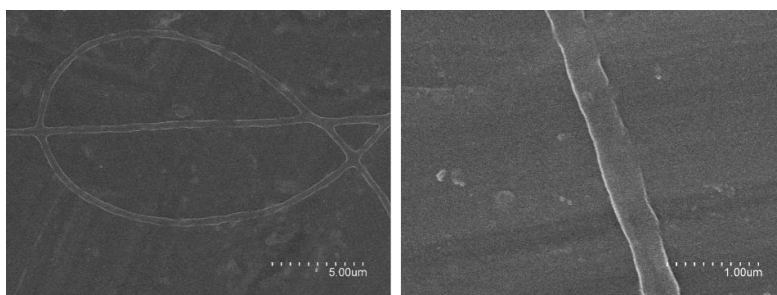


Figure 1. Micrographs of the structures obtained from jackfruit polyisoprenes dissolved in dichloromethane.

The images of the structures obtained with supporting polymers and PC are shown in (Figure 2). Micrographs of pullulan with 1% PC showed agglomerated fibers forming (Figure 2b). According to the dispersion stability, PC remains in suspension, and its accommodation in the fiber formation can be by adherence to the fiber shell, which causes the aggregation and flattening of film formation. Furthermore, it indicates that 1% of PC is a high concentration to be stabilized in 20% pullulan-aqueous solutions. Nanofibers' behavior and morphology with 1% PC are similar to those reported by Nie *et al.* [22], who evaluated the formation of *trans*-polyisoprene fibers ($M_n \approx 6.1 \times 10^4 \text{ g mol}^{-1}$, *trans*-1,4) by electrospinning. These authors associate fiber deformation with polyisoprenes' low glass transition temperature and the slow solidification process. Nanofibers with 0.5 and 0.2% PC revealed the formation of cylindrical-shaped continuous fibers without deformations or breaks and aggregations. These results are similar to those achieved with pullulan (Figure 2a-d), suggesting that at low PC concentrations, pullulan can maintain polyisoprenes stable. Muniz *et al.* [34] mention that the combination of polymers improves the mechanical, physical, thermal, and rheological properties observed in PC fibers with both polymers (PEO and pullulan).

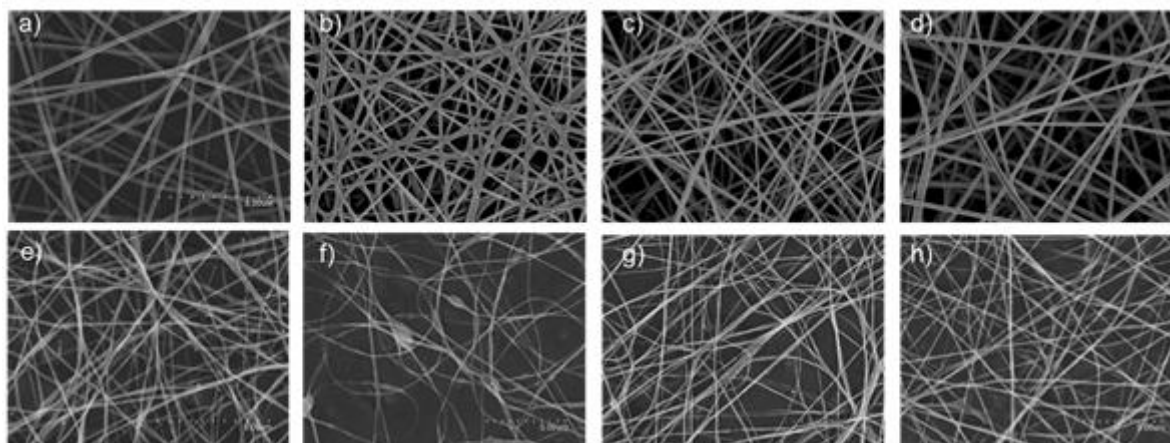


Figure 2. SEM micrographs of nanofibers. **a)** NF-PUL; **b)** NF-PUL-PC-1% ; **c)** NF-PUL-PC-0.5% ; **d)** NF-PUL-PC-0.2% ; **e)** NF-PEO; **f)** NF-PEO-PC-1% ; **g)** NF-PEO-PC-0.5% ; **h)** NF-PEO-PC-0.2% .

The micrographs corresponding to PEO structures show ultrafine fiber formation (100-200 nm), with small protrusions related to the high voltage applied during the electrospinning process and exhibiting a cylindrical shape (Figure 2 e). PC nanofibers showed slight changes in morphology, decreased protrusions caused by voltage, and did not exhibit agglomeration at any PC concentrations (Figure 2 f-h). The fiber morphology is similar to that reported by Song *et al.* [35], who fabricated PEO nanofibers by electrospinning; these authors obtained cylindrical, continuous, ultrafine, and smooth fibers without protuberances.

NF-PUL, NF-PUL-PC-0.5%, and NF-PUL-PC-0.2% nanofibers showed a diameter size distribution in the range from 200 to 400 nm, and the diameter increases with the

concentration of PC (Table 2). The average diameter of the highest frequency was 200-300 nm. These results are similar to those obtained by Aguilar-Vázquez *et al.* [36], who evaluated the fiber formation of pullulan by electrospinning; these authors obtained a mean diameter of 280 ± 47 nm. On the other hand, NF-PUL-PC-1% exhibits a wide size range of 200 to 600 nm (Figure 3). This could be explained due to the increase in the number of entanglements among the polymers caused by a higher PC concentration [37].

Table 2. Average size of nanofibers.

Nanofiber	Average size (nm)
NF-PUL	229 ± 22
NF-PUL-PC-0.2%	405 ± 6
NF-PUL-PC-0.5%	289 ± 5
NF-PUL-PC-1%	402 ± 10
NF-PEO	145 ± 29
NF-PEO-PC-0.2%	143 ± 22
NF-PEO-PC-0.5%	145 ± 20
NF-PEO-PC-1%	143 ± 26

With and without PC, PEO nanofibers exhibited homogeneity in size distribution, ranging from 100 to 300 nm. Fiber size agrees with the ones reported by Bizarria *et al.* [38], who produced PEO/chitosan fibers with diameters ranging from 50-300 nm. The difference between the diameters of PEO and pullulan nanofibers could be attributed to the polymers' polymer concentration, process stability, and rheological characteristics, including viscosity, flexibility, and elasticity [39]. PEO and pullulan proved to enhance the spinnability of PC and preserved the morphological characteristics of the fibers at room temperature.

3.3. Structure and chemical interactions of nanofibers.

The chemical structure of the produced materials was evaluated by ATR-FTIR to corroborate possible interactions with polyisoprenes. Pullulan exhibited a wide peak at 3,000 to 3,500 cm^{-1} corresponding to hydroxyl -OH group vibration. The vibration at 2,926 cm^{-1} corresponds to C-H elongation. Meanwhile, the peaks between 1,156 cm^{-1} and 1,028 cm^{-1} were assigned to C-O bonds (Figure 4a). Regarding PEO, the spectrum presents a pronounced peak in the 3,000 to 2,700 cm^{-1} band associated with C-H stretching. The C-O-C stretching was observed at 1,093 cm^{-1} . The peak at 960 cm^{-1} is related to the flexion of C-H₂ bond, and the vibration of C-H bond can be seen at 841 cm^{-1} . The chemical structure of the powders of both polymers agrees with the report by Vázquez-González *et al.* [40]. PC presented a peak in the band from 2,921 to 2,869 cm^{-1} associated with C-H₃ bonds and at 2,861 cm^{-1} related to C-H₂, corresponding to the functional groups of polyisoprenes. The band from 1,704 to 1,712 cm^{-1} belongs to the stretching of the C=C bonds, which is characteristic of *cis*-1,4 polyisoprene. The vibration at 980 cm^{-1} indicates C-H bending. These results agree with those reported by Ramos-Martinez *et al.* [8], who analyzed polyisoprenes from jackfruit latex.

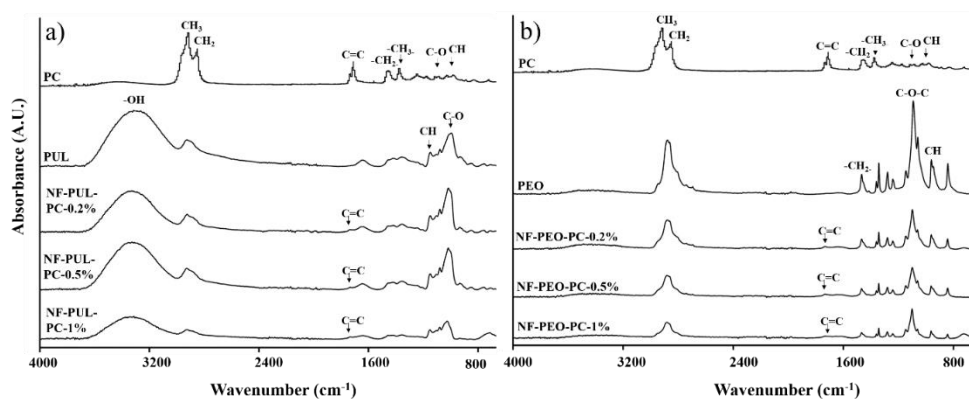


Figure 3. ATR-FTIR spectra of PEO and PUL are neat polymers in powder form, and nanofibers with PC use pullulan (NF-PUL-PC) and PEO (NF-PEO-PC) as supporting polymers.

The spectra of the PUL-PC nanofibers with the three concentrations (Figure 4a), manifested a decrease in the characteristic peaks of pullulan. Incorporating PC diminishes the intensity of the vibration associated with the hydroxyl groups in the band 3,500 to 2,700 cm^{-1} , a phenomenon associated with the interactions between polymers. Likewise, fibers with 1% of PC present the C=C double bond in the 1,704 cm^{-1} band, which is characteristic of polyisoprenes. It is important to note that as the concentration of PC in the nanofibers decreases, this peak is less noticeable; this phenomenon is related to the detection capacity of the equipment depending on the concentration sample. The spectrum of PEO-PC nanofibers shows no changes in the chemical structures (Figure 4b). A peak in the 1,704 cm^{-1} band that corresponds to the C=C double bond of polyisoprenes is observed in the fibers, suggesting the presence of PC in the fibers.

3.4. Water vapor transmission rate (WVTR) and solubility of nanofibers.

According to the morphology and distribution size, nanofibers with 0.5% PC with both polymers were selected to evaluate the physicochemical characteristics. The solubility of the nanostructures is an important factor in defining the potential application of new production processes in the industry. Nanofibers of both polymers, with and without PC, showed no statistical difference in any of the evaluated parameters ($p > 0.05$). This behavior could be attributed to the low percentages of PC incorporated. The solubility behavior of pullulan nanofibers is similar to that reported by Qin *et al.* [41] in pullulan fibers with chitosan. Meanwhile, the solubility value of nanofibers with PEO is similar to that reported by Rüzgar *et al.* [42] in fibers with PEO and curcumin (7.66 %).

Table 3. Water vapor transmission rate (WVTR) and solubility of nanofibers (NF).

Sample	WVTR ($\text{g}/\text{m}^2 \text{ day}$)	Solubility (%)
NF-PUL	415.01 ± 11.2 ^a	39.96 ± 3.5 ^a
NF-PUL-PC 0.5%	481.28 ± 21.6 ^a	34.54 ± 0.1 ^a
NF-PEO	413.69 ± 13.08 ^a	9.25 ± 0.1 ^a
NF-PEO-PC 0.5%	436.16 ± 14.95 ^a	8.67 ± 1.6 ^a

*Values expressed as mean ± standard deviation. Different letters per column and polymer indicate statistical difference $p < 0.05$.

3.5. Thermal stability of nanofibers.

NF-PUL-PC and NF-PUL showed a single mass variation attributed to the decomposition of the macromolecular chains of polymers and surfactant (Tween 20) in the temperature range of 284 to 325°C (Figure 5). NF-PUL-PC did not show the second mass variation, which, according to the PC thermogram, represents the decomposition of the oxidation products of polyisoprenes. This phenomenon can be explained by the results of ATR-FTIR analysis, which showed a decrease of the peaks in the band from 3,500 to 2,700 cm^{-1} that belong to the -OH groups of pullulan, due to their interaction with PC through the formation of hydrogen bonds. As a result, when they decompose, they break at the same temperature, which causes the overlapping of the decomposition temperature of the oxidation products (250 to 350°C) [43]. Also, a positive 50°C shift of the decomposition onset temperature of PC, when combined with pullulan, was observed. Moreover, when the sample is less pure, there is less chance of observing all stages of decomposition. NF-PEO-PC and NF-PEO also displayed a single mass variation from 353 to 395°C related to the decomposition of all its components. The polymer-polymer combination of PEO-PC shifted 150°C the onset of PC decomposition temperature, suggesting that cross-linking of the two polymers improves the thermal stability of polyisoprenes. The PC exhibits two mass variations (Figure 5); the first one is associated with the decomposition of the macromolecular chains of polyisoprenes (73.08%) and other compounds of lipidic character. The second variation (28%) is linked to thermal oxidation products of polyisoprenes (D-limonene), which decompose between 250 and 350°C [8].

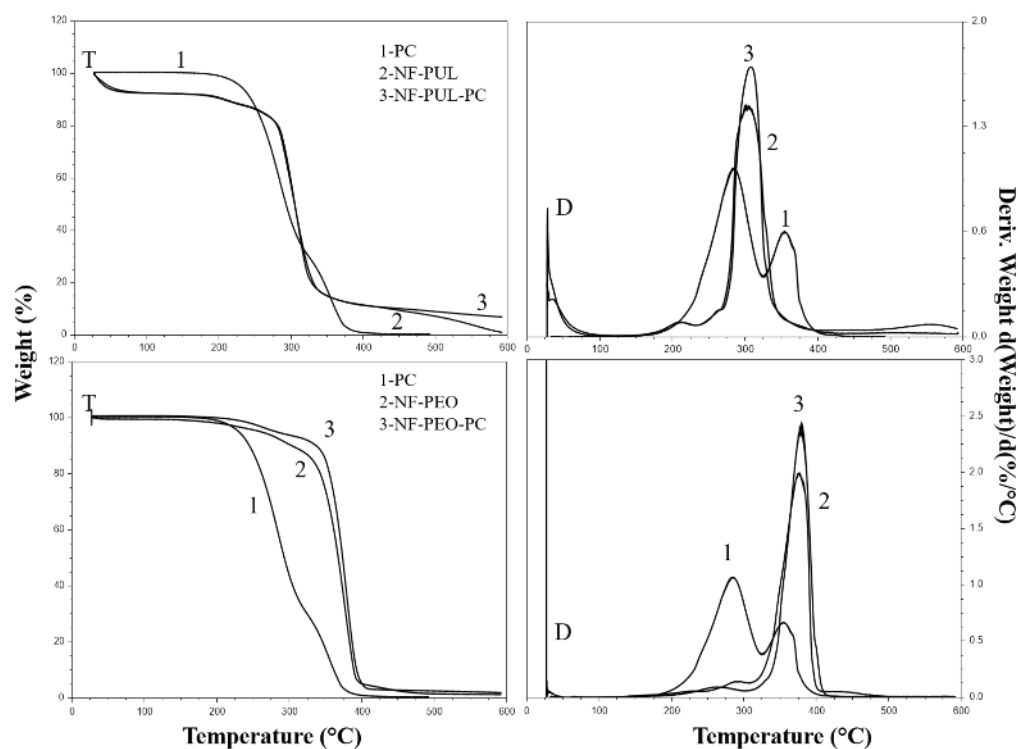


Figure 4. TGA thermograms (T) and derivatives curves (D) of polyisoprene concentrate (PC), pullulan nanofiber (NF-PUL), pullulan nanofiber with 0.5 of PC (NF-PUL-PC), PEO nanofiber (NF-PEO) and PEO nanofiber with 0.5 of PC (NF-PEO-PC).

Differential scanning calorimetry (DSC) is a convenient technique to investigate the miscibility between polymers and provides information about possible interactions between components and structural changes caused by the electrospinning process. The DSC thermogram of pullulans nanofiber exhibited a Tg temperature of 129.89°C, which was not

present on NF-PUL-PC (Figure 6b). A possible explanation could be that the glass transition temperature of jackfruit polyisoprenes is under -100°C , which could have caused a shift in the T_g when combined with PC [11]. Both nanofibers of pullulans (with and without PC) showed three thermal events; the first event at 146.68°C ($\Delta H 10.69 \text{ J g}^{-1}$) and 149.19°C ($\Delta H 17.94 \text{ J g}^{-1}$), respectively, related to the melting of monosaccharide residues. The second event occurred at 203.16°C ($\Delta H 97.78 \text{ J g}^{-1}$) for pullulan nanofiber without PC and 197.44°C ($\Delta H 60.59 \text{ J g}^{-1}$) for the pullulan nanofiber with PC, linked to polymeric chains melting of both polymers. A decrease in melting temperature and enthalpy was observed in NF-PUL-PC, suggesting a non-covalent interaction between the polymers (pullulan-polyisoprene). The lateral hydrogens of the polyisoprene molecule can bind by weak forces with pullulan carbonyl groups, a phenomenon that could have occurred during the heating of both polymers and the electrospinning process. The third endothermic event was observed close to 300°C for both nanofibers (with and without PC), related to the melting and decomposition of the macromolecular chains of the two polymers [37].

The DSC thermogram of NF-PEO-PC and REF-PEO displayed in cycle 2 a crystallization peak at 43.57°C ($\Delta H 84.45 \text{ J g}^{-1}$) and 42.29°C ($\Delta H 79.58 \text{ J g}^{-1}$), respectively (Figure 6c). In cycles 1 and 3, an endothermic peak ranged from 50 to 70°C for both samples, related to PEO melting [44]. In cycle 3, a crystallization peak appeared at 149°C , which was more evident in REF-PEO because of its pureness. The fourth event presents at 329.78°C for NF-PEO and at 367.46°C for NF-PEO-PC, which means a simultaneous event of melting and decomposition of macromolecular PEO chains.

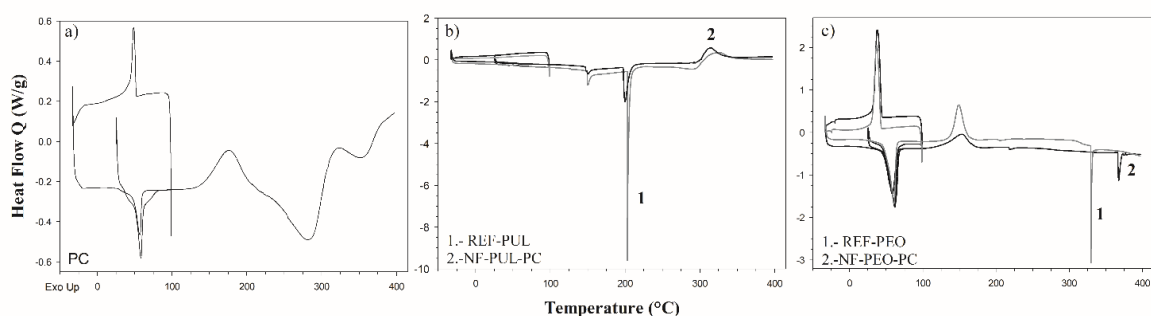


Figure 5. DSC thermograms a) polyisoprene concentrate (PC), b) Pullulan (NF-PUL) and pullulan nanofiber with 0.5 of PC (NF-PUL-PC), and c) PEO (NF-PEO) and PEO nanofiber with 0.5 of PC (NF-PEO-PC).

In neither of the nanofibers (NF-PEO-PC and NF-PUL-PC) was it possible to observe the characteristic crystallization and melting peaks of the polyisoprenes because the other polymeric materials are found in greater proportion (Figure 6). Polyisoprenes in both cis or trans conformations exhibit low glass transition and melting temperatures, which were observed in the DSC thermogram of the PC of jackfruit latex (Figure 6a). The thermal events of PC were previously reported by Ramos-Martinez *et al.* [8]. These authors observed an endothermic peak in the temperature range of 50 to 65°C in cycles 1 and 3, which is consistent with the results of this work.

4. Conclusions

The formation and production of low molecular weight polyisoprene nanofibers from jackfruit latex, pure and in combination with PEO and pullulan, by electrospinning, were achieved for the first time. Moreover, the PC nanofibers were in the nanometric range and showed adequate morphology. The physicochemical characterization of the nanofibers

revealed that polymer-polymer interactions are non-covalent, and the thermal stability of PC was increased. Nanofibers' solubility was relatively low, which guarantees good functionality during use. Nanofibers' applications are not limited and could be of great interest in various industrial areas such as food, biomedical, pharmaceutical, and nutricosmetics. However, based on the results of this study and the healing properties that have been attributed to polyisoprenes, an interesting and viable application is the fabrication of dermal patches.

Funding

CYTED thematic network code 319RT0576.

Acknowledgments

The authors thank CONACYT (Consejo Nacional de Ciencia y Tecnología-Mexico) for their support through scholarship number 801568 granted to Dania Marlene Ceballos Vázquez and Sabbatical Stay to Juan Arturo Ragazzo-Sanchez.

Conflicts of Interest

The authors assert that they have no conflicts of interest.

References

1. Khan, A.U.; Ema, I.J.; Faruk, M.R.; Tarapder, S.A.; Khan, A.U.; Noreen, S.; Adnan, M. A Review on Importance of *Artocarpus Heterophyllus* L. (Jackfruit). *J. Multidiscip. Appl. Nat. Sci.* **2021**, *1*, <http://doi.org/10.47352/jmans.v1i2.88>.
2. Wagner, I.; Lackner, M. Extraction and Analysis of Natural Rubber from the Latex of *Ficus carica*, *Artocarpus heterophyllus* and Polymer Analysis of *Durio zibethinus*. *Austin J. Biotechnol. Bioeng.* **2021**, *8*, 1112, <http://doi.org/10.26420/austinjbiotechnolbioeng.2021.1112>.
3. Guerra, N.B.; Pegorin, G.S.; Boratto, M.H.; de Barros, N.R.; de Oliveira Graeff, C.F.; Herculano, R.D. Biomedical Applications of Natural Rubber Latex from the Rubber Tree *Hevea Brasiliensis*. *Mater. Sci. Eng. C* **2021**, *126*, 112126, <https://doi.org/10.1016/j.msec.2021.112126>.
4. Pegorin, G.S.; Leite, M.N.; Antoniassi, M.; Chagas, A.L.D.; Santana, L.A.; Garms, B.C.; Marcelino, M.Y.; Herculano, R.D.; Frade, M.A.C. Physico-chemical characterization and tissue healing changes by *Hancornia speciosa* Gomes latex biomembrane. *J. Biomed. Mater. Res. - Part B Appl. Biomater.* **2021**, *109*, 938– 948, <https://doi.org/10.1002/jbm.b.34758>.
5. Rosa, S.D.S.R.F.; Rosa, M.F.F.; Fonseca, M.A.M.; Luz, G.V.D.S.; Avila, C.F.D.; Domínguez, A.G.D.; Dantas, A.G.D.; Richter, V.B. Evidence in Practice of Tissue Healing with Latex Biomembrane: Integrative Review. *J. Diabetes Res.* **2019**, *2019*, 7457295, <https://doi.org/10.1155/2019/7457295>.
6. Benjamaa, R.; Moujanni, A.; Kaushik, N.; Choi, E.H.; Essamadi, A.K.; Kaushik, N.K. *Euphorbia* species latex: A comprehensive review on phytochemistry and biological activities. *Front. Plant Sci.* **2022**, *13*, 1008881, <http://doi.org/10.3389/fpls.2022.1008881>.
7. Hernandez-Hernandez, A.B.; Alarcon-Aguilar, F.J.; Garcia-Lorenzana, M.; Rodriguez-Monroy, M.A.; Canales-Martinez, M.M. *Jatropha Neopauciflora* Pax Latex Exhibits Wound-Healing Effect in Normal and Diabetic Mice. *J. Evidence-Based Integr. Med.* **2021**, *26*, <http://doi.org/10.1177/2515690X20986762>.
8. Ramos-Martínez, O.; González-Cruz, E.M.; Calderón-Santoyo, M.; Ragazzo-Sánchez, J.A. Polyisoprenes obtained from jackfruit latex (*Artocarpus heterophyllus* L.): Extraction and characterization. *J. Appl. Polym. Sci.* **2022**, *139*, e52392, <https://doi.org/10.1002/app.52392>.
9. Gracz-Bernaciak, J.; Mazur, O.; Nawrot, R. Functional Studies of Plant Latex as a Rich Source of Bioactive Compounds: Focus on Proteins and Alkaloids. *Int. J. Mol. Sci.* **2021**, *22*, 12427, <http://doi.org/10.3390/ijms222212427>.
10. Li, R.; Wang, Z.; Lian, X.; Hu, X.; Wang, Y. Antimicrobial Rubber Nanocapsule-Based Iodophor Promotes Wound Healing. *CCS Chem.* **2020**, *2*, 245–256, <https://doi.org/10.31635/ccschem.020.201900101>.
11. Bhadra, S.; Mohan, N.; Parikh, G.; Nair, S. Possibility of artocarpus heterophyllus latex as an alternative source for natural rubber. *Polym. Test.* **2019**, *79*, 106066, <https://doi.org/10.1016/j.polymertesting.2019.106066>.
12. Lin, T.-C.; Yang, C.-Y.; Wu, T.-H.; Tseng, C.-H.; Yen, F.-L. Myricetin Nanofibers Enhanced Water Solubility and Skin Penetration for Increasing Antioxidant and Photoprotective Activities. *Pharmaceutics*

- 2023**, *15*, 906, <http://doi.org/10.3390/pharmaceutics15030906>.
13. Al-Abduljabbar, A.; Farooq, I. Electrospun Polymer Nanofibers: Processing, Properties, and Applications. *Polymers* **2023**, *15*, 65, <http://doi.org/10.3390/polym15010065>.
 14. He, X.; Wang, L.; Lv, K.; Li, W.; Qin, S.; Tang, Z. Polyethylene Oxide Assisted Fish Collagen-Poly-ε-Caprolactone Nanofiber Membranes by Electrospinning. *Nanomaterials* **2022**, *12*, 900, <http://doi.org/10.3390/nano12060900>.
 15. Amjadi, S.; Gholizadeh, S.; Ebrahimi, A.; Almasi, H.; Hamishehkar, H.; Taheri, R.A. Development and characterization of the carvone-loaded zein/pullulan hybrid electrospun nanofibers for food and medical applications. *Ind. Crops Prod.* **2022**, *183*, 114964, <http://doi.org/10.1016/j.indcrop.2022.114964>.
 16. Van den Eynde, K.; Boon, V.; Gaspar, R.C.; Fardim, P. Biofabrication of Functional Pullulan by *Aureobasidium pullulans* under the Effect of Varying Mineral Salts and Sugar Stress Conditions. *Molecules* **2023**, *28*, 2478, <http://doi.org/10.3390/molecules28062478>.
 17. Angel, N.; Li, S.; Yan, F.; Kong, L. Recent advances in electrospinning of nanofibers from bio-based carbohydrate polymers and their applications. *Trends Food Sci. Technol.* **2022**, *120*, 1308-324, <http://doi.org/10.1016/j.tifs.2022.01.003>.
 18. Peinado, I.; Mason, M.; Romano, A.; Biasioli, F.; Scampicchio, M. Stability of β-carotene in polyethylene oxide electrospun nanofibers. *Appl. Surf. Sci.* **2016**, *370*, 111–116, <http://doi.org/10.1016/j.apsusc.2016.02.150>.
 19. Lorente, M.Á.; González-Gaitano, G.; González-Benito, J. Preparation, Properties and Water Dissolution Behavior of Polyethylene Oxide Mats Prepared by Solution Blow Spinning. *Polymers* **2022**, *14*, 1299, <http://doi.org/10.3390/polym14071299>.
 20. Chen, Q.; Saha, P.; Kim, N.G.; Kim, J.K. Processing and characterization of electrospun trans-polyisoprene nanofibers. *J. Polym. Eng.* **2015**, *35*, 53–59, <https://doi.org/10.1515/polyeng-2014-0124>.
 21. Hao, X.; Bai, C.; Huang, Y.; Bi, J.; Zhang, C.; Cai, H.; Zhang, X.; Du, L. Preparation of cis-1,4-Polyisoprene Electrospun Microfibers. *Macromol. Mater. Eng.* **2010**, *295*, 305–309, <https://doi.org/10.1002/mame.200900284>.
 22. Nie, H.R.; Wang, C.; He, A.H. Fabrication and chemical cross-linking of electrospun trans-polyisoprene nanofiber nonwoven. *Chinese J. Polym. Sci.* **2016**, *34*, 697–708, <http://doi.org/10.1007/s10118-016-1796-2>.
 23. Shao, H.F.; Li, Z.L.; He, A.H.; Liu, C.G.; Yao, W. Fabrication of trans-1,4-polyisoprene nanofibers by electrospinning and its crystallization behavior and mechanism. *Chinese J. Polym. Sci.* **2016**, *34*, 797–804, <http://doi.org/10.1007/s10118-016-1797-1>.
 24. Dognani, G.; da Silva, A.A.; Cabrera, F.C.; Fanta, F.L.; Saénz, C.A.T.; Bechtold, I.H.; Job, A.E.; Agostini, D.L.D.S. Electrospun natural rubber fibers-based flexible conductive membranes. *Matéria(Rio de Janeiro)* **2020**, *25*, <https://doi.org/10.1590/S1517-707620200003.1116>.
 25. Jimenez-Sánchez, D.E.; Calderón-Santoyo, M.; Ortiz-Basurto, R.I.; Bautista-Rosales, P.U.; Ragazzo-Sánchez, J.A. Effect of maltodextrin reduction and native agave fructans addition on the physicochemical properties of spray-dried mango and pineapple juices. *Food Sci. Technol. Int.* **2018**, *24*, 519–532, <http://doi.org/10.1177/1082013218769168>.
 26. González-Estrada, R.R.; Calderón-Santoyo, M.; Ragazzo-Sánchez, J.A.; Peyron, S.; Chalier, P. Antimicrobial soy protein isolate-based films: physical characterisation, active agent retention and antifungal properties against *Penicillium italicum*. *Int. J. Food Sci. Technol.* **2018**, *53*, 921–929, <http://doi.org/10.1111/ijfs.13664>.
 27. Medeiros, G.B.; Lima, F.d.A.; de Almeida, D.S.; Guerra, V.G.; Aguiar, M.L. Modification and Functionalization of Fibers Formed by Electrospinning: A Review. *Membranes* **2022**, *12*, 861, <http://doi.org/10.3390/membranes12090861>.
 28. González-Cruz, E.M.; Calderón-Santoyo, M.; Barros-Castillo, J.C.; Ragazzo-Sánchez, J.A. Evaluation of Evaluation of biopolymers in the encapsulation by electrospraying of polyphenolic compounds extracted from blueberry (*Vaccinium corymbosum* L.) variety Biloxi. *Polym. Bull.* **2021**, *78*, 3561–3576, <http://doi.org/10.1007/s00289-020-03292-3>.
 29. Gagaoua, M.; Pinto, V.Z.; Göksen, G.; Alessandroni, L.; Lamri, M.; Dib, A.L.; Boukid, F. Electrospinning as a Promising Process to Preserve the Quality and Safety of Meat and Meat Products. *Coatings* **2022**, *12*, 644, <http://doi.org/10.3390/coatings12050644>.
 30. Jia, X.W.; Qin, Z.Y.; Xu, J.X.; Kong, B.H.; Liu, Q.; Wang, H. Preparation and characterization of pea protein isolate-pullulan blend electrospun nanofiber films. *Int. J. Biol. Macromol.* **2020**, *157*, 641–647, <http://doi.org/10.1016/j.ijbiomac.2019.11.216>.
 31. Ponrasu, T.; Chen, B.H.; Chou, T.H.; Wu, J.J.; Cheng, Y.S. Fast Dissolving Electrospun Nanofibers Fabricated from Jelly Fig Polysaccharide/Pullulan for Drug Delivery Applications. *Polymers* **2021**, *13*, 241, <http://doi.org/10.3390/polym13020241>.
 32. Calabrò, E.; Magazù, S. Demicellization of Polyethylene Oxide in Water Solution under Static Magnetic Field Exposure Studied by FTIR Spectroscopy. *Adv. Phys. Chem.* **2013**, *2013*, 485865, <https://doi.org/10.1155/2013/485865>.
 33. Ali, Z.; Din, F.U.; Zahid, F.; Sohail, S.; Imran, B.; Khan, S.; Malik, M.; Zeb, A.; Khan, G.M. RETRACTED ARTICLE: Transdermal delivery of allopurinol-loaded nanostructured lipid carrier in the treatment of gout. *BMC Pharmacol. Toxicol.* **2022**, *23*, 86, <http://doi.org/10.1186/s40360-022-00625-y>.

34. Muniz, N.O.; Vechietti, F.A.; Anesi, G.R.; Guinea, G.V.; Dos Santos, L.A.L. Blend-based fibers produced via centrifugal spinning and electrospinning processes: Physical and rheological properties. *J. Mater. Res.* **2020**, *35*, 2905–2916, <http://doi.org/10.1557/jmr.2020.189>.
35. Song, Z.; Chiang, S.W.; Chu, X.; Du, H.; Li, J.; Gan, L.; Xu, C.; Yao, Y.; He, Y.; Li, B.; Kang, F. Effects of solvent on structures and properties of electrospun poly(ethylene oxide) nanofibers. *J. Appl. Polym. Sci.* **2018**, *135*, 45787, <http://doi.org/10.1002/app.45787>.
36. Aguilar-Vázquez, G.; Loarca-Piña, G.; Figueroa-Cárdenas, J.D.; Mendoza, S. Electrospun fibers from blends of pea (*Pisum sativum*) protein and pullulan. *Food Hydrocoll.* **2018**, *83*, 173–181, <https://doi.org/10.1016/j.foodhyd.2018.04.051>.
37. Poudel, D.; Swilley-Sanchez, S.; O'keefe, S.; Matson, J.; Long, T.; Fernández-Fraguas, C. Novel Electrospun Pullulan Fibers Incorporating Hydroxypropyl- β -Cyclodextrin: Morphology and Relation with Rheological Properties. *Polymers* **2020**, *12*, 2558, <http://doi.org/10.3390/polym12112558>.
38. Bizarría, M.T.M.; d'Ávila, M.A.; Meil, L.H.I. Non-woven nanofiber chitosan/peo membranes obtained by electrospinning. *Brazilian J. Chem. Eng.* **2014**, *31*, 57–68, <http://doi.org/10.1590/S0104-66322014000100007>.
39. Ebagninin, K.W.; Benchabane, A.; Bekkour, K. Rheological characterization of poly(ethylene oxide) solutions of different molecular weights. *J. Colloid Interface Sci.* **2009**, *336*, 360–367, <http://doi.org/10.1016/j.jcis.2009.03.014>.
40. Vázquez-González, Y.; Prieto, C.; Stojanovic, M.; Torres, C.A.V.; Freitas, F.; Ragazzo-Sánchez, J.A.; Calderón-Santoyo, M.; Lagaron, J.M. Preparation and Characterization of Electrospun Polysaccharide FucoPol-Based Nanofiber Systems. *Nanomaterials* **2022**, *12*, 498, <http://doi.org/10.3390/nano12030498>.
41. Qin, Z.Y.; Jia, X.W.; Liu, Q.; Kong, B.H.; Wang, H. Fast dissolving oral films for drug delivery prepared from chitosan/pullulan electrospinning nanofibers. *Int. J. Biol. Macromol.* **2019**, *137*, 224–231, <http://doi.org/10.1016/j.ijbiomac.2019.06.224>.
42. Rüzgar, G.; Birer, M.; Tort, S.; Acartürk, F. Studies on Improvement of Water-Solubility of Curcumin with Electrospun Nanofibers. *Fabad J. Pharm. Sci.* **2013**, *38*, 143–149.
43. Dony, P.; Berzin, F. Thermogravimetric, Morphological and Infrared Analysis of Blends Involving Thermoplastic Starch and Poly(ethylene-co-methacrylic acid) and Its Ionomer Form. *Molecules* **2023**, *28*, 4519, <http://doi.org/10.3390/molecules28114519>.
44. Maccaferri, E.; Ortolani, J.; Mazzocchetti, L.; Benelli, T.; Brugo, M.T.; Zucchelli, A.; Giorgini, L. New Application Field of Polyethylene Oxide: PEO Nanofibers as Epoxy Toughener for Effective CFRP Delamination Resistance Improvement. *ACS Omega* **2022**, *7*, 23189–23200, <http://doi.org/10.1021/acsomega.2c01189>.